

planes make a dihedral angle of 11.0°, and these interactions appear weaker than those observed in the [Cu(L-glu)(*o*-phen)H₂O]·3H₂O complex,² where the dihedral angle between aromatic ring planes is 1.4°.

The complex is stable in air and presents a thermogravimetric behavior corresponding to the loss of uncoordinated and coordinated water molecules in the 35–120 °C temperature range. In the square-pyramidal [Cu(L-glu)(*o*-phen)H₂O]·3H₂O complex² the coordinated water molecule is lost in the 110–150 °C temperature range, indicating a greater bond strength of the coordinated water molecule in a square-pyramidal than in a tetragonally distorted octahedral environment.

The room-temperature magnetic moment of the complex ($\mu_{\text{eff}}(293 \text{ K}) = 1.84 \mu_{\text{B}}$) is "normal" and typical of "magnetically dilute" complexes;²¹ its polycrystalline EPR spectrum ($g_{\parallel} = 2.33$; $g_{\perp} = 2.08$) closely resembles those of copper(II) complexes having similar environments and chromophores, reported in the literature,^{21,22} for which an essentially $d_{x^2-y^2}$ ground state has been suggested.

The room-temperature electronic spectrum of the complex presents a broad d-d band with an unsymmetrical maximum centered at 16 400 cm⁻¹, typical of CuN₃O₃ chromophores.^{23,24}

Acknowledgment. We are grateful to the Centro di Calcolo Elettronico dell'Università di Modena for computing support and to the Centro Strumenti dell'Università di Modena for recording EPR spectra.

Registry No. [Cu(L-asp)(*o*-phen)H₂O]·4H₂O, 102649-32-1.

Supplementary Material Available: Listings of atomic temperature factors, hydrogen atom parameters, complete bond distances and angles, hydrogen-bonding distances and angles, ring-stacking interactions, and selected least-squares planes (7 pages). Ordering information is given on any current masthead page.

- (21) Hathaway, B. J.; Billing, D. E. *Coord. Chem. Rev.* **1970**, *5*, 143.
 (22) Hathaway, B. J. *Struct. Bonding (Berlin)* **1984**, *57*, 55 and references cited therein.
 (23) Freeman, H. C.; Guss, G. M.; Healy, M. J.; Martin, R. P.; Nockolde, C. E.; Sarkar, B. J. *J. Chem. Soc., Chem. Commun.* **1969**, 225.
 (24) Yamauchi, O.; Sakurai, T.; Nakahara, A. *J. Am. Chem. Soc.* **1979**, *101*, 4164.

Contribution from the Laboratory
 of Analytical Chemistry, Faculty of Science,
 Nagoya University, Chikusa, Nagoya 464, Japan

Kinetic Study of Acetic Acid Exchange on Manganese(II), Cobalt(II), and Copper(II) Acetates in Acetic Acid by Oxygen-17 Nuclear Magnetic Resonance¹

Akiharu Hioki,[†] Shigenobu Funahashi,* and Motoharu Tanaka

Received October 2, 1985

We have previously studied acetic acid exchange on perchlorates of manganese(II), iron(II), cobalt(II), nickel(II), and copper(II) ions in acetic acid (HOAc).² These metal(II) perchlorates in acetic acid exist as hexasolvometal ions that form ion pairs with perchlorate anion. On the other hand, acetate ion (OAc⁻) in transition-metal(II) acetates is bound to the central metal ions in acetic acid.^{3,4} Thus, we expect that coordinated acetate ion exerts some effect on the solvent-exchange rate, i.e., bound-ligand effect. In this work rates of acetic acid exchange on Mn(OAc)₂, Co(OAc)₂, and Cu₂(OAc)₄ (tetrakis(μ -acetato)dycopper(II)) in acetic acid and mixtures with dichloromethane-*d*₂ as an inert cosolvent were measured by means of the oxygen-17 NMR line-broadening method. The activation parameters obtained are

compared with those for the corresponding perchlorates.²

Experimental Section

The purification of acetic acid and dichloromethane-*d*₂ (CD₂Cl₂) and the preparation of oxygen-17-enriched acetic acid were described previously.^{2,5-8} The percentage of oxygen-17 in the oxygen-17-enriched acetic acid is 5.13 atom % of all oxygen atoms. The mean molecular weight of this oxygen-17-enriched acetic acid is 60.53. Tetrasolvometal manganese(II) acetate was prepared by adding the stoichiometric amount of acetic anhydride to the tetrahydrate dissolved in acetic acid and allowing the reaction to occur at room temperature for 2 weeks.⁴ The obtained crystal was washed with acetic anhydride and acetic acid. The resultant pale pink compound may be formulated as Mn(OAc)₂(HOAc)₄. The compound, dried in a desiccator over sodium hydroxide for 1 week under reduced pressure, should be Mn(OAc)₂(HOAc), which was confirmed by the analysis for manganese (calcd, 23.57%; found, 23.55%). Hydrated cobalt(II) acetate (reagent grade) was recrystallized from distilled water. The hydrate was dissolved in acetic acid. In order to eliminate the water, excess acetic anhydride was added to the cobalt(II) acetate solution. After this solution was allowed to stand at 80 °C for 3 days, anhydrous cobalt(II) acetate precipitated. This red crystal was recrystallized from acetic acid and may be formulated as Co(OAc)₂(H-OAc)₄. The crystals were dried at 120 °C for 3 h to obtain Co(OAc)₂. The quantitative change of Co(OAc)₂(HOAc)₄ to Co(OAc)₂ was confirmed thermogravimetrically (Shimadzu thermal analyzer DT-30). Tetrakis(μ -acetato)dycopper(II) disolvate (Cu₂(OAc)₄(HOAc)₂, dimeric copper(II) acetate) was prepared as described previously.⁵ It was dried in a desiccator over sodium hydroxide for a few days under a reduced pressure. The determination of copper in the dried copper(II) acetate crystals by both electrolysis and EDTA titration confirmed the composition of Cu₂(OAc)₄.

¹⁷O NMR spectra were obtained with use of JNM-FX60, JNM-FX90QE, and JNM-GX400 (JEOL Ltd.) instruments operating at 8.16, 12.15, and 54.21 MHz, respectively. ¹H NMR spectra were observed at 60 MHz on a JNM-C-60H NMR spectrometer (JEOL Ltd.). The preparation of NMR samples and the NMR measurement have been described in our previous paper.⁸ The compositions of samples for the NMR measurement are tabulated in Table I.

The temperature dependence of the observed transverse relaxation rate, $1/T_{2p}$, corrected for the ligand relaxation rate in the absence of the metal complex, can be analyzed by the modified Swift and Connick equation (eq 1),⁹⁻¹¹ where symbols have the usual meaning.⁸ The analysis of data was carried out by the least-squares program SALS.¹²

$$(T_{2p}P_M)^{-1} = \frac{1}{\tau_M} \frac{T_{2M}^{-2} + (\tau_M T_{2M})^{-1} + (\Delta\omega_M)^2}{(\tau_M^{-1} + T_{2M}^{-1})^2 + (\Delta\omega_M)^2} + \frac{1}{T_{20}} \quad (1)$$

Results

All NMR data for line broadening are tabulated in Tables s-I and s-II (supplementary material).

Manganese(II) Acetate. The temperature dependence of line widths $\log(T_{2p}P_M)^{-1}$ for manganese(II) acetate is represented in Figure 1. It is reasonable that the chemical-exchange region, where τ_M^{-1} contributes to the line width to a large extent, is identical at 8.16, 12.15, and 54.21 MHz for the sample of 20.4 wt % HOAc. NMR and kinetic parameters for a nonlinear least-squares fitting are given in Table s-III (supplementary

- (1) Metal Complexes in Acetic Acid. 9. For part 8: see ref 2.
 (2) Hioki, A.; Funahashi, S.; Ishii, M.; Tanaka, M. *Inorg. Chem.* **1986**, *25*, 1360-1364.
 (3) Hendriks, C. F.; van Beek, H. C. A.; Heertjes, P. M. *Ind. Eng. Chem. Prod. Res. Dev.* **1979**, *18*, 43-46.
 (4) Kolling, O. W.; Lambert, J. L. *Inorg. Chem.* **1964**, *3*, 202-205.
 (5) Funahashi, S.; Nishimoto, T.; Hioki, A.; Tanaka, M. *Inorg. Chem.* **1981**, *20*, 2648-2651.
 (6) Sawada, K.; Ohtaki, H.; Tanaka, M. *J. Inorg. Nucl. Chem.* **1972**, *34*, 625-636.
 (7) Hioki, A.; Funahashi, S.; Tanaka, M. *Inorg. Chem.* **1983**, *22*, 749-752.
 (8) Hioki, A.; Funahashi, S.; Tanaka, M. *J. Phys. Chem.* **1985**, *89*, 5057-5061.
 (9) Swift, T. J.; Connick, R. E. *J. Chem. Phys.* **1962**, *37*, 307-320.
 (10) Luz, Z.; Meiboom, S. *J. Chem. Phys.* **1964**, *40*, 1058-1066.
 (11) Rusnak, L. L.; Jordan, R. B. *Inorg. Chem.* **1976**, *15*, 709-713.
 (12) Nakagawa, T.; Oyanagi, Y. "SALS" (statistical analysis with least-squares fitting), Program Library, Nagoya University Computation Center, 1979.

[†] Present address: The National Chemical Laboratory for Industry, Yatabe, Ibaraki 305, Japan.

Table I. Compositions of Sample Solutions

soln	species	[M]/m ^a	[HOAc]/m	[CD ₂ Cl ₂]/m	P _M	wt % of HOAc
A0	ref soln	0	16.52	0	0	100.0
A1m	Mn(OAc) ₂	4.84 × 10 ⁻³	16.52	0	8.78 × 10 ⁻⁴	100.0
A2o	Co(OAc) ₂	1.44 × 10 ⁻²	16.52	0	2.62 × 10 ⁻³	100.0
A3u	Cu ₂ (OAc) ₄	1.11 × 10 ^{-2b}	16.52	0	6.75 × 10 ⁻⁴	100.0
A4u	Cu ₂ (OAc) ₄	2.30 × 10 ^{-2b}	16.52	0	1.40 × 10 ⁻³	100.0
B0	ref soln	0	3.37	9.16	0	20.4
B1m	Mn(OAc) ₂	2.30 × 10 ⁻⁴	3.37	9.16	2.06 × 10 ⁻⁴	20.4
B2o	Co(OAc) ₂	3.32 × 10 ⁻³	3.37	9.16	2.97 × 10 ⁻³	20.4
B3o	Co(OAc) ₂	6.63 × 10 ⁻³	3.37	9.16	5.96 × 10 ⁻³	20.4
B4u	Cu ₂ (OAc) ₄	2.74 × 10 ^{-2b}	3.37	9.16	8.25 × 10 ⁻³	20.4
B5u	Cu ₂ (OAc) ₄	2.95 × 10 ^{-2b}	3.37	9.16	8.90 × 10 ⁻³	20.4
B6u	Cu ₂ (OAc) ₄	4.72 × 10 ^{-2b}	3.37	9.16	1.44 × 10 ⁻²	20.4
C0 ^c	ref soln	0	0.79	11.0	0	4.8
C1m ^c	Mn(OAc) ₂	1.96 × 10 ⁻⁴	0.79	11.0	9.87 × 10 ⁻⁴	4.8

^a m is in the unit of mol kg⁻¹. ^b Concentration as dimer for Cu₂(OAc)₄. ^c Solution C was used for measuring the hydroxyl proton NMR.

Table II. Rate Constants and Activation Parameters for Acetic Acid Exchange

metal species	ΔH [‡] /kJ mol ⁻¹	ΔS [‡] /J mol ⁻¹ K ⁻¹	k(25 °C)/s ⁻¹	concn of HOAc/wt %	remarks
Mn(OAc) ₂	32 ± 3	9 ± 11	(4.8 ± 0.9) × 10 ⁷	20.4	this work
Mn(ClO ₄) ₂	29 ± 2	-10 ± 7	(1.6 ± 0.1) × 10 ⁷	4.94, 20.0, 100	ref 2 (¹⁷ O)
Co(OAc) ₂	37 ± 3	14 ± 12	(9.9 ± 3.3) × 10 ⁶	20.4	this work
Co(ClO ₄) ₂	37 ± 3	-6 ± 12	(1.3 ± 0.2) × 10 ⁶	20.0	ref 2 (¹⁷ O)
Cu ₂ (OAc) ₄	51 ± 5	18 ± 15	(6.3 ± 1.0) × 10 ⁴	100	this work
Cu ₂ (OAc) ₄	51 ± 2	12 ± 6	(2.8 ± 0.1) × 10 ⁴	20.4	this work
Cu ₂ (OAc) ₄	53 ± 4	13 ± 8	(1.7 ± 0.2) × 10 ⁴	24.1	ref 5 (¹ H (CH ₃))
Cu ₂ (OAc) ₄	51 ± 4	3 ± 8	(1.2 ± 0.2) × 10 ⁴	9.8	ref 5 (¹ H (CH ₃))
Cu ₂ (OAc) ₄	53 ± 4	10 ± 8	(9.4 ± 1.1) × 10 ³	4.3	ref 5 (¹ H (CH ₃))
Cu(ClO ₄) ₂			≈ 1 × 10 ^{7a}	4.94, 20.0	ref 2 (¹⁷ O)

^a At -25 °C.

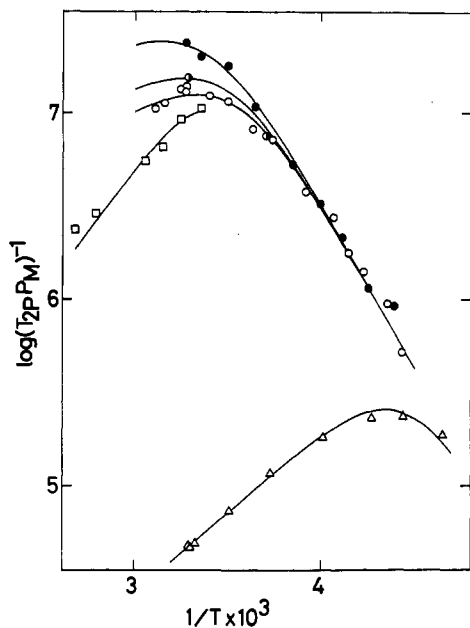


Figure 1. Temperature dependence of $\log(T_{2p}P_M)^{-1}$ for the hydroxyl proton and the oxygen-17 of bulk acetic acid in the presence of Mn(OAc)₂: □, oxygen-17 of solution A1m at 8.16 MHz; ○, oxygen-17 of solution B1m at 8.16 MHz; ●, solution B1m at 12.15 MHz; ●, solution B1m at 54.21 MHz; Δ, hydroxyl proton of solution C1m at 60.0 MHz. The curves in Figures 1–3 were calculated with the NMR and kinetic parameters obtained.

material). The rate constants and activation parameters obtained are summarized in Table II. For the sample of 100 wt % HOAc the contribution of chemical exchange to $\log(T_{2p}P_M)^{-1}$ is relatively small due to the relatively high freezing point (16.6 °C) of acetic acid. However, these data are consistent with the activation parameters obtained for the sample of 20.4 wt % HOAc. Data of the hydroxyl proton for the sample of 4.8 wt % HOAc seem

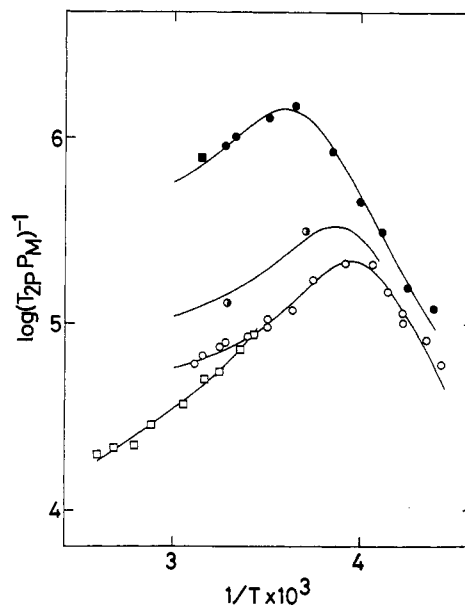


Figure 2. Temperature dependence of $\log(T_{2p}P_M)^{-1}$ for the oxygen-17 of bulk acetic acid in the presence of Co(OAc)₂: □, solution A2o at 8.16 MHz; ■, solution A2o at 54.21 MHz; ○, solutions B2o and B3o at 8.16 MHz; ●, solution B3o at 12.15 MHz; ●, solution B3o at 54.21 MHz.

also to agree satisfactorily with the activation parameters obtained by ¹⁷O NMR.

For oxygen-17 NMR at the higher temperature range $1/T < 3.5 \times 10^{-3} \text{ K}^{-1}$, the value of $\log(T_{2p}P_M)^{-1}$ at 54.21 MHz is larger than that at 8.16 MHz. Since the T_{2M}^{-1} term for oxygen-17 is attributable to the hyperfine interaction, the longitudinal relaxation time of the electron depends on the observed frequency as in the case of Mn(ClO₄)₂.^{2,10,13}

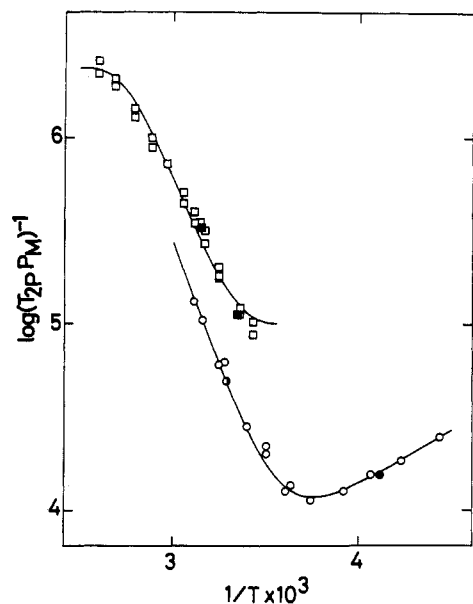


Figure 3. Temperature dependence of $\log(T_{2p}P_M)^{-1}$ for the oxygen-17 of bulk acetic acid in the presence of $\text{Cu}_2(\text{OAc})_4$: \square , solutions A3u and A4u at 8.16 MHz; \blacksquare , solution A3u at 54.21 MHz; \circ , solutions B4u, B5u, and B6u at 8.16 MHz; \bullet , solution B4u at 12.15 MHz; \ominus , solution B6u at 54.21 MHz.

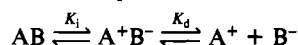
Cobalt(II) Acetate. The temperature dependence of line widths $\log(T_{2p}P_M)^{-1}$ of ^{17}O NMR for cobalt(II) acetate is presented in Figure 2. Data at 12.15 MHz are not inconsistent with the activation parameters (given in Table II) obtained for the other two observed frequencies (8.16 and 54.21 MHz). For the sample solution of 100 wt % HOAc the chemical-exchange region was not observed above the freezing point of the solution (16.6 °C). No ^1H NMR line broadening was observed within the limited solubility of $\text{Co}(\text{OAc})_2$.

At the higher temperature range $1/T < 4 \times 10^{-3} \text{ K}^{-1}$ the line widths depend greatly on the frequencies. This results from the contribution of $\Delta\omega_M$. The scalar coupling constant (A/\hbar) is calculated to be $4.6 \times 10^7 \text{ rad s}^{-1}$.

Copper(II) Acetate Dimer. In Figure 3 is given the temperature dependence of line widths of ^{17}O NMR for the copper(II) acetate dimer. τ_M^{-1} and T_{2O}^{-1} do not depend on observed frequencies at all. The activation parameters for the acetic acid exchange on the copper(II) acetate dimer are listed in Table II together with those obtained by ^1H NMR.⁵

Discussion

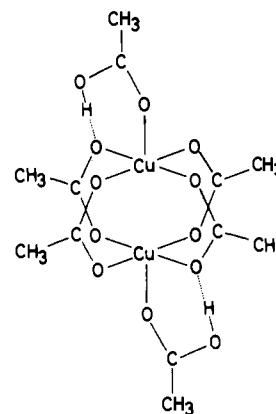
In acetic acid with low dielectric constant, we should consider separately the ionization and dissociation steps. Dissociation of the 1:1 electrolyte AB is expressed as



Overall dissociation constants $K_D (= [\text{A}^+][\text{B}^-]/([\text{AB}] + [\text{A}^+\text{B}^-]) = K_i K_d / (1 + K_i))$ for metal(II) acetates ($\text{M}(\text{OAc})_2 \rightleftharpoons \text{M}(\text{OAc})^+ + \text{OAc}^-$) are available.⁴ K_D values are $10^{-7.53} \text{ mol dm}^{-3}$ for $\text{Mn}(\text{OAc})_2$ and $10^{-7.56} \text{ mol dm}^{-3}$ for $\text{Co}(\text{OAc})_2$. K_d is calculated to be about $10^{-6} \text{ mol dm}^{-3}$ for these 1:1 electrolytes by an equation of the type derived by Fuoss and Kraus.¹⁴ Judging from the K_i values, which are estimated to be $10^{-1.53}$ for $\text{Mn}(\text{OAc})_2$ and $10^{-1.56}$ for $\text{Co}(\text{OAc})_2$, it may be concluded that two OAc^- ions in each acetate salt exist in the inner sphere of the metal(II) ion. This is also supported by our studies on the equilibria and kinetics of some metal(II) acetates in acetic acid.^{6,15-17} From vapor pressure measurements, the van't Hoff coefficients of the manganese(II)

and cobalt(II) acetates were determined to be unity and that of copper(II) acetate was one-half.¹⁵ Therefore, copper(II) acetate exists as a dimer, while the other acetates are monomeric in acetic acid. Solubilities of manganese(II) and cobalt(II) acetates were measured to investigate the aquation of these metal acetates, and the equilibrium of copper(II) acetate with water was studied by cryoscopy.¹⁵ Judging from these findings, there is no effect of H_2O under the present experimental conditions, because the amount of water in the present systems is at most less than $10^{-3} \text{ mol kg}^{-1}$. The equilibrium constants for reaction of copper(II) acetate with hydrochloric acid, perchloric acid, lithium chloride, and lithium acetate were determined by means of spectrophotometry.^{6,16} Kinetic studies on reactions of the copper(II) acetate dimer with lithium chloride and hydrogen chloride have elucidated their reaction mechanisms.¹⁷ The strongest acid is perchloric acid although it forms an ion pair in acetic acid. The addition of the stoichiometric amount of HClO_4 to the $\text{M}(\text{OAc})_2$ solution gives the corresponding $\text{M}(\text{ClO}_4)_2$ solution.

There have been some studies on the monomer-dimer equilibrium of copper acetate as a function of the water concentration in acetic acid.¹⁷⁻¹⁹ Under our experimental conditions copper(II) acetate should exist solely as a dimer. According to Grasdalen,²⁰ in ethanol solution the ethanol molecules coordinated to the dimeric copper acetate at its axial position are readily replaced by addition of acetic acid. This is contrary to the prediction based on the difference in the basicity between acetic acid and ethanol: the latter is much more basic than the former. Moreover, in the ^1H NMR spectra of mixed solvents involving both ethanol and acetic acid in the presence of the dimeric copper acetate, the ethanol signals are the same as those of pure ethanol while the HOAc signals are very broad and shifted. These facts point to a strong interaction of acetic acid with the copper species. The geometry should thus favor the coordination of acetic acid by an extra hydrogen bonding with the bridging acetate as I.



I

As apparent from Table II, the exchange rates for $\text{Mn}(\text{OAc})_2$ and $\text{Co}(\text{OAc})_2$ are obviously higher than those for $\text{Mn}(\text{ClO}_4)_2$ and $\text{Co}(\text{ClO}_4)_2$, respectively. This enhancement of exchange rate seems to result from an electron donation from coordinated acetate ions to the central metal(II) ion.²¹

As can be seen from Table II, the activation parameters for acetic acid exchange on the copper(II) acetate dimer obtained from ^{17}O NMR are in good agreement with those from ^1H NMR reported previously,⁵ although the acetic acid concentration ranges from 4.3 wt % (0.72 mol kg^{-1}) to 100 wt % (17 mol kg^{-1}). As proposed previously,⁵ this solvent exchange corresponds to acetic acid exchange with a dissociative activation mode at the axial sites of tetrakis(μ -acetato)dycopper(II). The solvent exchange on

(14) Fuoss, R. M.; Kraus, C. A. *J. Am. Chem. Soc.* **1933**, *55*, 1019-1028.

(15) Sawada, K.; Tanaka, M. *J. Inorg. Nucl. Chem.* **1973**, *35*, 2455-2464.

(16) Sawada, K.; Ohtaki, H.; Tanaka, M. *J. Inorg. Nucl. Chem.* **1972**, *34*, 3455-3466.

(17) Funahashi, S.; Nishimoto, T.; Banerjee, P.; Sawada, K.; Tanaka, M. *Bull. Chem. Soc. Jpn.* **1980**, *53*, 1555-1559.

(18) Cheng, A. T. A.; Howald, R. A. *Inorg. Chem.* **1975**, *14*, 546-549.

(19) Grasdalen, H.; Svare, I. *Acta Chem. Scand.* **1971**, *25*, 1089-1102.

(20) Grasdalen, H. *Acta Chem. Scand.* **1971**, *25*, 1103-1113.

(21) Tanaka, M.; Yamada, S. *J. Chem. Soc., Chem. Commun.* **1976**, 178-179.

hexasolventocopper(II) ion in acetic acid is very fast, as expected from the Jahn-Teller effect of the copper(II) ion,² while the solvent-exchange rate on the copper acetate is much slower, since the latter forms the dimeric structure and the solvated acetic acid molecules at its axial sites are stabilized by hydrogen bonding as depicted in I.

Acknowledgment. The present work was supported through a Grant-in-Aid for Scientific Research (No. 59430010) and a Grant-in-Aid for Special Project Research (No. 60129031) from the Japanese Ministry of Education, Science, and Culture.

Registry No. HOAc, 64-19-7; Mn(OAc)₂, 638-38-0; Co(OAc)₂, 71-48-7; Cu₂(OAc)₄, 23686-23-9.

Supplementary Material Available: Oxygen-17 line-broadening data for Mn(OAc)₂, Co(OAc)₂, and Cu₂(OAc)₄ in acetic acid and in mixtures with CD₂Cl₂ (Table s-I), proton line-broadening data for Mn(OAc)₂ in an acetic acid-CD₂Cl₂ mixture (Table s-II), and values of ΔH^\ddagger , ΔS^\ddagger , C_M , E_M , C_O , E_O , and C_w (Table s-III) (5 pages). Ordering information is given on any current masthead page.

Contribution from the Department of Chemistry,
University of Hamburg, D-2 Hamburg 13, FRG

Ring-Substituted Derivatives of η^5 -C₅H₅V(CO)₄: Synthesis and ⁵¹V NMR Spectroscopic Characteristics

Martin Hoch, Andreas Duch, and Dieter Rehder*

Received February 12, 1986

In a recent paper,¹ Basolo and co-workers described the synthesis and molecular structure of η^5 -C₉H₇V(CO)₄ (**1**) (C₉H₇ = indenyl), obtained in 40% yield from the reaction of [V(CO)₆]⁻ and C₉H₇HgCl. We have found that the direct action of the neutral 17-electron complex V(CO)₆ on indene produces **1** in about 70% yield. This reaction, which possibly runs via an intermediate "HV(CO)₆",² can more generally be applied to the synthesis of other ring-substituted cyclopentadienyl complexes in yields of 55-85% and thus opens a route to this little known class of compounds alternative to the hydride transfer from phosphine-stabilized hydridocarbonylvanadium complexes to the exocyclic carbon of pentafulvenes.³ Ring-substituted derivatives of C₅-H₅V(CO)₄ are of considerable interest in the context of the stabilization of the labile C₅H₅V(CO)₃THF, an excellent precursor for the synthesis of a large variety of substitution products C₅H₅V(CO)₃L.⁴

Experimental Section

All operations were carried out under nitrogen and in oxygen-free, absolute solvents. Bis(cyclopentadienes), as far as available commercially ((C₅H₆)₂, (C₅Me₅)₂, (C₅(Et)Me₄H)₂, (C₅Me₃H)₂) and indene were purified by distillation. Silica gel (Kieselgel 60, Merck, 10-230 mesh ASTM) was pretreated in vacuo (8 h, 1-2 Torr) and loaded with N₂.

Preparation of Alkylcyclopentadienes. The equivalent of 2.4 g of sodium hydride (77 mmol) of a paraffin oil suspension of NaH was washed twice with 20-mL portions of light petroleum ether, dried in vacuo, treated with 100 mL of THF, and cooled in an ice bath. A 77-mmol sample (ca. 5 g or 6.4 mL) of freshly distilled C₅(R)H₅ (R = H, Me) was added so as to keep the evolution of H₂ at a moderate rate. In case the solution was still turbid, further cyclopentadiene was added in small portions until clearing. To this colorless to pink solution was added 65 mmol of alkyl halide (CyBr or CyCl, (cetyl)Br, (trityl)Cl). After ca. 2 h of refluxing, the yellow to light red solution was evaporated, the remaining oil or paste redissolved in 100 mL of diethyl ether, and the resultant solution washed four times with 10-mL portions of water. The

Table I. Yields and Selected Properties of η^5 -Cp'V(CO)₄ Complexes

complex	Cp' ^a	yield, %	properties
1	indenyl	69	orange crystals
2	C ₅ (trityl)H ₄	85	yellow crystals
3	C ₅ Me ₅	73	orange powder
4	C ₅ (Et)Me ₄	72	orange powder
5	C ₅ Me(cetyl)H ₃	58	light yellow wax
6	C ₅ Me(Cy)H ₃	54	orange crystals
7	C ₅ MeH ₄	76	orange oil

^a Abbreviations: indenyl = C₉H₇, trityl = C(C₆H₅)₃, cetyl = n-C₁₆H₃₃, Cy = c-C₆H₁₁.

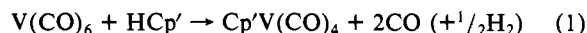
organic phase was then dried over MgSO₄ and the ether removed by distillation. Workup of the residual products was carried out by fractional distillation (C₅Me(Cy)H₄, 80-85 °C at 15-18 Torr; yield 60%), by filtration of the ether solution through a 6-cm layer of silica gel (C₅Me(cetyl)H₃;⁵ yield 85%), or by recrystallization from petroleum ether⁶ (C₅(trityl)H₃; yield 85%). Only the cyclohexyl derivative tends to dimerize.

V(CO)₆ was obtained in 91% yields by reacting 9-g portions of Na-(diglyme)₂V(CO)₆ (Ventron) with 18 g of orthophosphoric acid, intimately mixed in a sublimation apparatus. V(CO)₆ sublimes from this mixture at 50 °C and 0.01 Torr.

η^5 -Cp'V(CO)₄. In a typical experiment, 310 mg (1.4 mmol) of V(CO)₆, dissolved in 25 mL of *n*-hexane, was treated with 1.7 mmol of the freshly distilled cyclopentadiene and the mixture refluxed for 2 h. Direct sunlight was avoided. In *n*-pentane, reaction times are about 3 times as long. Small amounts of vanadium metal and [Cp'₂V(CO)₂][V(CO)₆] were filtered off. The filtrate, appearing orange or green (the latter due to suspended vanadium particles) and containing Cp'V(CO)₄ and (HCp')_n (¹H NMR evidence), was evaporated to yield an oil. This was dissolved in 1 mL of THF and chromatographed on silica gel with pentane as elutant (column dimensions 10 × 25 cm; ca. 60 mL of pentane; elution time ca. 1 h). After removal of the pentane by vacuum evaporation at room temperature, the complexes were obtained in a pure form and with satisfactory elemental analyses. Yields and some of the properties of the new compounds are given in Table I.

Results and Discussion

The compounds described in this work and obtained according to eq 1 are given in Table II together with their characteristic vanadium-51 NMR shifts and CO stretching frequencies. In



contrast to findings on (acetyl-C₅H₄)V(CO)₄⁷ and various (alkenyl-C₅H₄)V(CO)₄ complexes,^{2, 3, 4, 6, and 7} show two IR-active bands only. The B₁ mode, which should gain intensity as the overall C_{4v} symmetry of the parent cyclopentadienyl complex decreases, arises as a weak shoulder in the case of **1**, **2**, and **5**. No splitting of the E mode⁷ was observed. The absence of the B₁ band in most of the complexes Cp'V(CO)₄ shows that the effective local symmetry is still C_{4v}; i.e. there are no rotational barriers for Cp' at room temperature. Complexes **1**, **4**, and **5** have also been characterized by their mass spectra,⁸ showing a frag-

(5) $n^{18.5}_D$ 1.4702; melting range 10-14 °C.

(6) Hartmann, H.; Flenner, K.-H. *Z. Phys. Chem. (Liepzig)* **1950**, *194*, 278.

(7) Palyi, G.; King, R. B. *Inorg. Chim. Acta* **1975**, *15*, L23.

(8) Selected peaks, *m/e* (relative intensities in parentheses), are as follows: (indenyl)V(CO)₄: 278 (7), C₉H₇V(CO)₄: 250 (10), C₉H₇V(CO)₃: 222 (12), C₉H₇V(CO)₂: 194 (10), C₉H₇V(CO): 166 (100), C₉H₇: 140 (11), C₇H₅V: 115 (24), C₉H₇: 89 (7), C₉H₅: 76 (7), C₅H₄: 65 (15), C₅H₃: {(Et)Me₄C₅V(CO)₄: 312 (52), (Et)Me₄CpV(CO)₄: 284 (46), (Et)Me₄(CpV(CO)₃): 256 (31), (Et)Me₄CpV(CO)₂: 228 (68), (Et)Me₄CpV(CO): 200 (100), (Et)Me₄CpV: 185 (45), possibly η -C₆Me₅H₅V: 184 (90), likely corresponding to [η^6 -C₆Me₅H₅]V, a plausible fragment of [(η^6 -arene)V(CO)₄]⁺ (Calderazzo, F.; Pampaloni, G.; Vitale, D.; Zanazzi, P. F. *J. Chem. Soc., Dalton Trans.* **1982**, 1993); 51 (65), V; metastable peaks 175.4 (EtMe₄CpV(CO)⁺ → EtMe₄CpV⁺ + CO), 169.3 (EtMe₄CpV⁺ → C₆Me₅HV⁺ + CH₄). [(Me(cetyl)H₃C₅)V(CO)₄: 466 (2), Me(cetyl)CpV(CO)₄: 438 (1), Me(cetyl)CpV(CO)₃: 410 (1), Me(cetyl)V(CO)₂: 382 (2), Me(cetyl)V(CO): 354 (43), Me(cetyl)V: 303 (100), Me(cetyl)Cp: 70 (7), C₅H₁₀: 56 (41), C₄H₈: 42 (79), C₃H₄. The following peaks correspond to the fragmentation pattern of the cetyl fragment c-[C₃(Me)H](CH₂)₃CH₃ (*n* and the relative intensities are given in parentheses): 178 (*n* = 9; 2), 164 (*n* = 8; 6), 150 (*n* = 7; 7), 136 (*n* = 6; 16), 122 (*n* = 5; 23), 108 (*n* = 4; 77), 94 (*n* = 3; 80).

(1) Kowalewski, R. M.; Kipp, D. O.; Stauffer, K. J.; Swepston, P. N.; Basolo, F. *Inorg. Chem.* **1985**, *24*, 3750.

(2) Hoffmann, K.; Weiss, E. *J. Organomet. Chem.* **1977**, *131*, 273.

(3) Wenke, D.; Rehder, D. *J. Organomet. Chem.* **1984**, *273*, C43.

(4) Hoch, M.; Rehder, D. *J. Organomet. Chem.* **1985**, *288*, C25.